NOTES AND CORRESPONDENCE

Low-Level Cloud Features and Airflow of an Oklahoma Hailstorm

RANDALL R. BENSCH AND JOHN MCCARTHY

Department of Meteorology, University of Oklahoma, Norman 73019

31 May 1977 and 5 January 1978

ABSTRACT

The low-level airflow and thermodynamic features of an Oklahoma hailstorm are explored using single-Doppler radar data and research aircraft measurements. Cloud structures at the base of the hailstorm are matched with the airflow in that part of the thunderstorm. A distinct discontinuity in the thermodynamic properties of the air reveals the existence of an outflow boundary in the form of a weak gust front. The nature of the airflow in the area of the gust front indicates that much of the inflow air is ascending over the gust frontal surface as it enters the storm updrafts.

1. Introduction

The low-level features of severe thunderstorms have long been of interest, not only with regard to fundamental dynamic structure, but to surface and aviation hazard considerations as well. Recently, several multiple-Doppler radar studies such as Brandes (1977), Heymsfield (1978) and Ray (1976) have produced a variety of results, centering on kinematic and airflow features. Unfortunately, the fine-detail structures (<1 km) of the airflow, particularly in the vicinity of the gust front, usually are not seen due to the limiting effect of the large sampling volume of the radar system. Using a tall instrumented tower, Goff (1976) has presented a rather detailed description of gust front structure, but little work has been done to merge these fine-scale wind and thermodynamic data to Doppler data. Furthermore, the mobility of an instrumented aircraft offers a significant advantage over a fixed tower, as well as a substantially improved space-time resolution. This work attempts to merge both Doppler radar and aircraft data to delineate the low-level thermodynamic and airflow features of a severe hailstorm, with particular emphasis on gust front features.

2. Observations on hailstorm

On the afternoon of 13 June 1975 a thunderstorm in northcentral Oklahoma produced hailstones as large as 7.5 cm in diameter. This hailstorm formed at about 1305,[1] rapidly intensified between 1315 and 1345, then reached its most intense stage during the time period 1400–1445. After 1445, the storm weakened. Fig. 1 shows the storm motion over about 30 min time increments as obtained from the National Severe Storms Laboratory (NSSL) WSR-57 radar located at Norman, Okla. The 0° elevation angle maximum reflectivity center is used as a reference point for storm position. The radar history and storm motion vectors are shown for 1332 to 1458 with first echo at 1305 indicated.

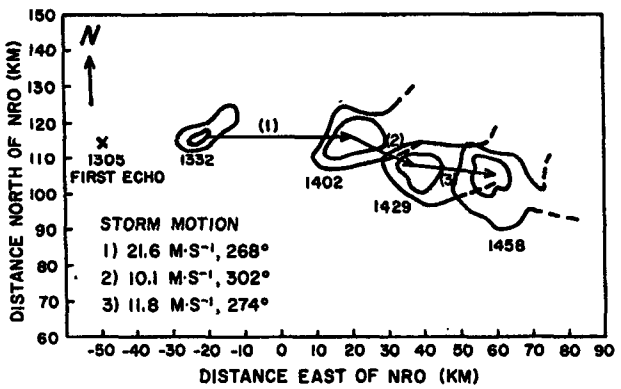

FIG. 1. The radar history and 30 min mean storm motion vectors for the time period 1332–1458 CST 13 June 1975, taken from WSR-57 radar film data. First echo is indicated for 1305. The outer contour of reflectivity is 27 dBZ and the inner contour 42 dBZ. Average vector storm motion is shown for three periods.

Visual and photographic evidence indicates that a well-organized updraft region existed on the southwest edge of the afternoon hailstorm[2] during the period 1400–1500. A long, tapered inflow cloud commonly known as a "tail" cloud extended from the storm toward the southwest and later toward the south. Below the main cloud base, a persistent lowering of the cloud base known as a "wall" cloud existed (after Fujita, 1957).

[1] All times CST.

[2] So called to distinguish it from an evening tornadic storm in nearly the same location.

0027-0644/78/0566-0571$05.00

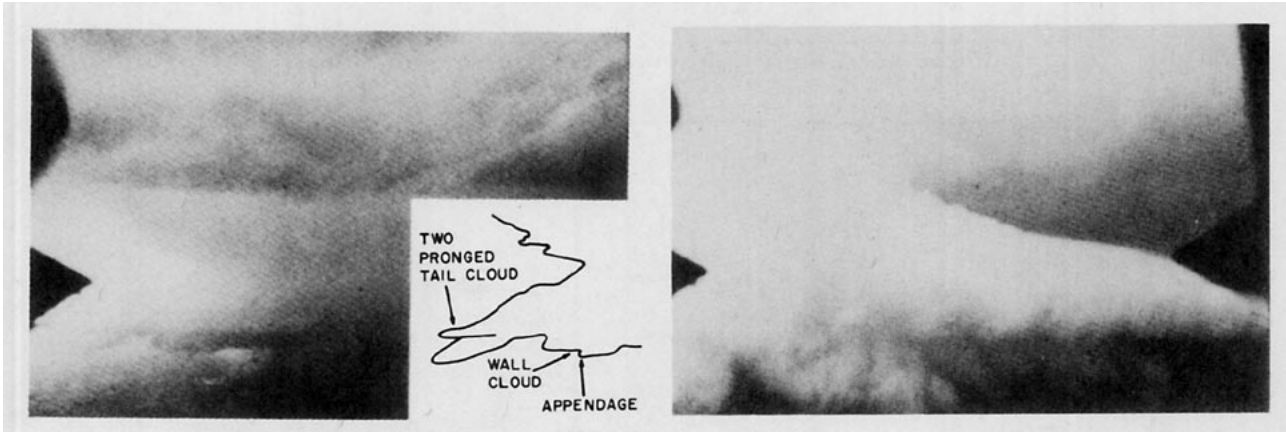

FIG. 2a. Overall view of the afternoon hailstorm at 1443 CST, looking toward about 320°. The insert at the lower right labels the cloud features in the lower left part of the photograph.

FIG. 2b. The tail cloud at 1448 CST looking toward about 70°.

Below the wall cloud a small funnel-like appendage was evident for more than 5 min after 1435. No tornado or true funnel formed although cyclonic rotation was observed in the wall cloud by several competent observers[3].

Fig. 2a is a broad view of the lower part of the hailstorm at about 1443 looking toward ~320° from the National Center for Atmospheric Research (NCAR) 306D research aircraft. Although this time is somewhat later than the times for which aircraft and radar data will be examined[4], it does clearly show the persis-

[3] These included Mr. Rick Bellatti, a Civil Defense Storm Spotter of Stillwater, Okla., and Mr. Gene Moore and Mr. Michael Watts, meteorology students and experienced storm interceptors (private communications).

[4] The photographs used in Fig. 2 were chosen at the later time since earlier photographs did not have a good overall perspective.

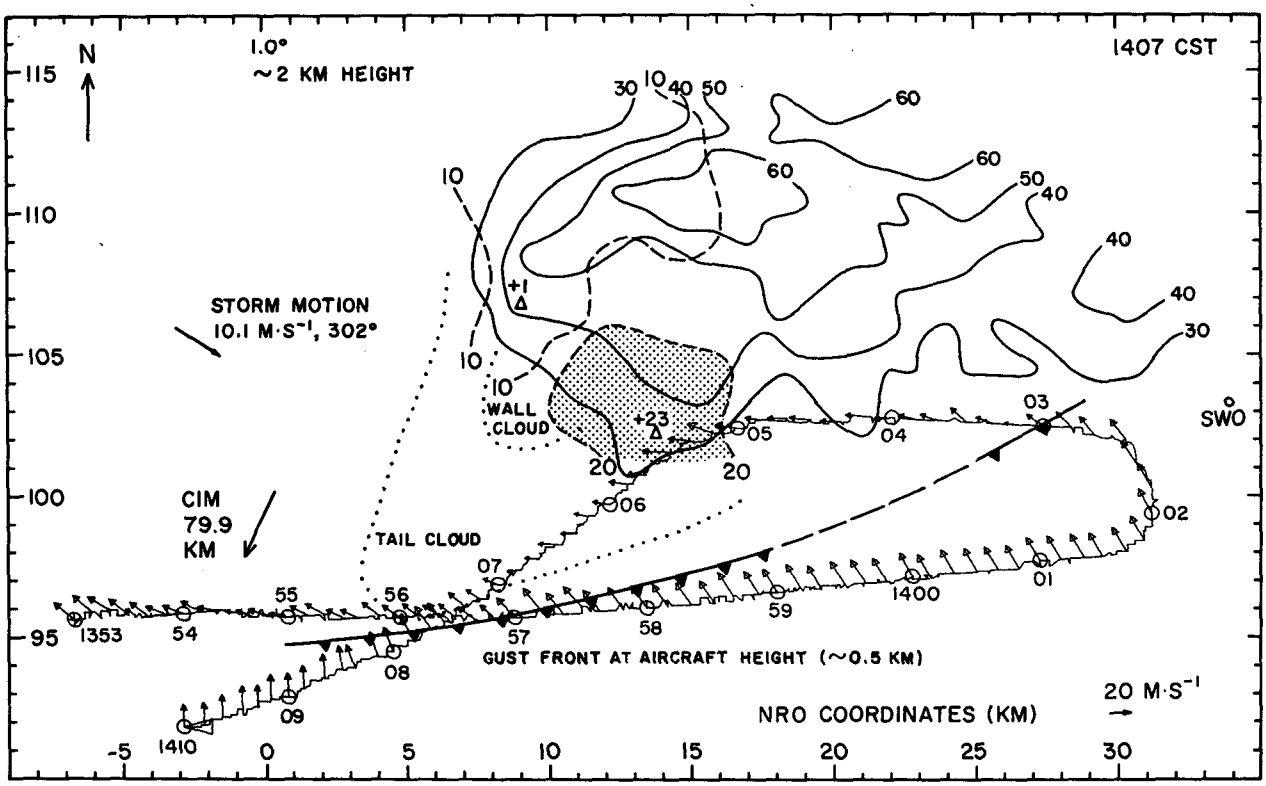

FIG. 3. Cimarron Doppler radar 1.0° elevation angle reflectivity (solid contours, dBZ) and radial velocities (corrected for storm motion) at 1407 CST. The maximum and minimum values of radial velocity are indicated by the Δ symbols with the numerical values shown. The area of radial velocities greater than 20 m s^{-1} is shaded. The NCAR research aircraft storm relative track and wind vectors are shown for 1353–1410. The inflow cloud as determined from aircraft photography is shown. SWO indicates the location of the Stillwater Municipal Airport.

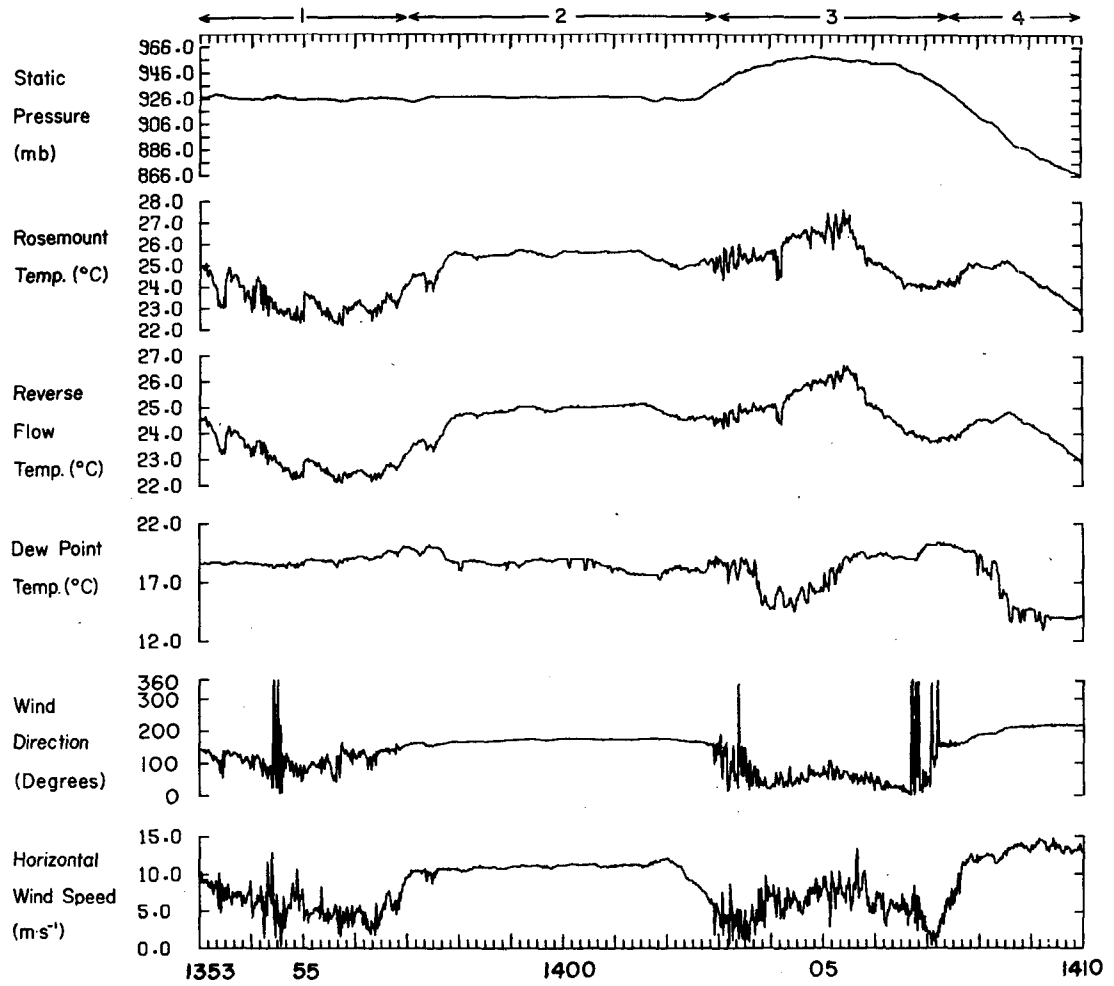

tent cloud features that had existed earlier as well. The tail cloud is clearly evident extending toward the left in the photograph. The tail cloud ends in two "prongs," one of which is lower and to the east of the other; both are labeled in Fig. 2. An examination of the variation of equivalent potential temperature as a function of distance from the storm suggests the lower prong may be produced by air that originates very near the surface, and from a position quite close to the inflow-outflow boundary, while the upper prong also is formed by surface air, but which arrives at the storm from a significantly greater distance. The lower prong air presumably had a higher moisture content originally than did the upper prong. In Fig. 2a the wall cloud is clearly seen below the main cloud base. The small funnel-like appendage is also visible. Heavy precipitation exists in the dark area to the right in the photograph. Hail up to 5 cm in diameter had fallen at the Stillwater Municipal Airport (SWO) a few minutes earlier at 1433[5]. Fig. 2b is a closer view of the tail cloud from the west side looking toward approximately 70° at about 1448. The double "prong" nature of the tail cloud is again evident. The thunderstorm had begun to weaken by this time, but the cloud features are still prominent.

The radar and research aircraft presentation to be discussed is for a time earlier than that shown in Fig. 2. Single-Doppler radar data from the NSSL Cimarron Doppler radar (CIM) were used in an analysis[6] for about a 1 min period centered at 1407. Fig. 3 shows the 1.0° elevation angle (~2 km AGL) presentation of the CIM radar reflectivity and *storm relative* radial velocities (storm motion 10.1 m s^{-1} from 302°) for 1407. Positive values of radial velocity indicate motion away from the radar; negative values indicate motion toward the radar with the storm motion component removed. Notice the strong reflectivity core (>60 dBZ reflectivity) and the tongue of high reflectivity extending toward the right-rear (west) part of the storm. The minimum radial velocity lies at the end of the high

[5] Taken from *Storm Data and Unusual Weather Phenomena*; accuracy of time unknown.

[6] Single-Doppler analysis technique provided by Mr. E. A. Brandes of NSSL.

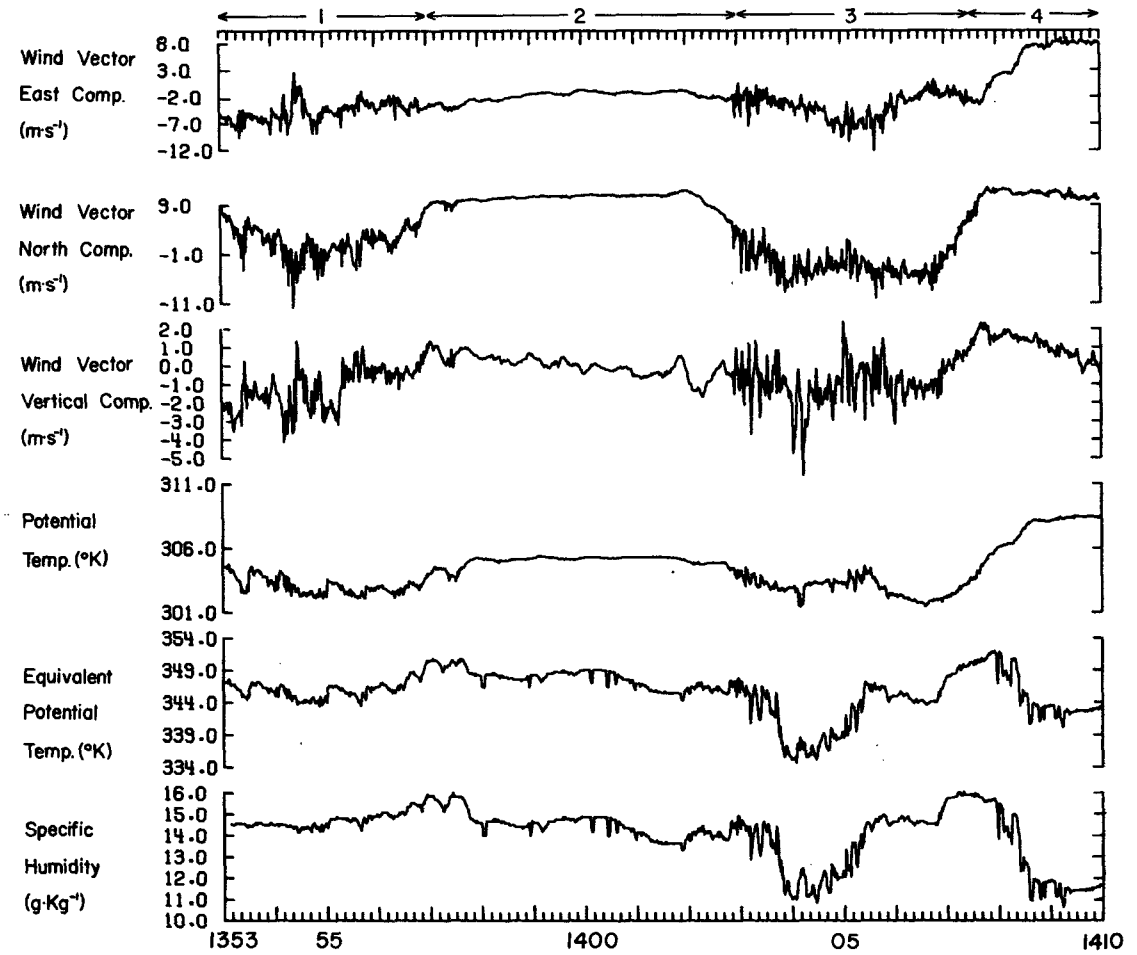

FIG. 4. Aircraft traces of pressure, Rosemount temperature, reverse flow temperature, dew-point temperature, ground relative wind direction, horizontal wind speed, horizontal (north and east) and vertical wind components, potential temperature, equivalent potential temperature and specific humidity for 1353–1410 CST. Winds in Fig. 4 are ground relative. Those in Fig. 3 are storm relative. Positive north and east wind components indicate winds toward these directions.

reflectivity tongue with an area of substantial (>20 m s^{-1}) positive radial velocities to the front of it. This suggests cyclonic airflow in this region.

Two additional features are included in Fig. 3. These are the outlines of the inflow cloud features and the research aircraft storm relative track for the time period 1353–1410 with *storm relative* wind vectors. The cloud outlines were determined from time lapse photographs taken from the aircraft. We believe that this merging of visual features with the quantitative airflow features is important to a clearer understanding of cloud formation, as well as providing a more coherent picture to aid in severe storm spotting. The aircraft track is shown on this figure to show its position relative to the storm. The aircraft did not maintain a completely constant altitude, but was in all cases less than 1 km AGL so the wind vectors do not correspond to the winds at the 2 km level represented in the single-Doppler analysis.

Fig. 4 shows the aircraft traces of pressure, temperature, dew point, ground relative wind components, potential temperature, equivalent potential temperature and specific humidity for the time period 1353–1410, which correspond to the aircraft track shown in Fig. 3. The 1353–1410 aircraft track can be divided into four segments according to airflow and thermodynamic properties: these are 1) 1353–1357, outflow air near the leading edge of the weak gust front discontinuity [this air is cool and moist with east to occasionally northeast ground relative wind components (see Fig. 4)]; 2) 1357–1403, pure inflow air [this air is warm and moist with southeast ground relative wind components]; 3) 1403:00–1407:30, outflow air along the edge of the precipitation shaft [the equivalent potential temperature drops to 335 K and the ground relative wind has a northerly component]; and 4) 1407:30–1410:00, inflow updraft air [the equivalent potential temperature rises briefly to 352 K as the aircraft skirts the edge of the main updraft at 1407:50 where sustained updraft speeds of 2 m s^{-1} are observed].

The air in segment 2 is very similar in its temperature

and moisture properties to relatively undisturbed air near the surface, sampled by the aircraft earlier at a position some distance from the storm. In segments 1 and 3, the air varies greatly in its thermodynamic properties indicating considerable mixing, in contrast to the laminar-flow unmixed inflow air in segment 2. The minimum value of the equivalent potential temperature in segment 3 of 335 K corresponds to undiluted air from the 1.5 km AGL level as sampled by the aircraft in the near environment of the storm.

Several aspects of the three-dimensional airflow and thermodynamic properties of the storm can be seen when Figs. 3 and 4 are studied. A "gust front" has been drawn in on Fig. 3 following the indications of its position from the aircraft measurements. It appears that this gust front is rather shallow. Evidence for this includes the fact that air to the north is generally moving away from the frontal boundary in the *storm relative* reference frame. Goff (1976) found that the airflow in the upper part of the outflow is actually away from the frontal boundary in the *gust front relative* frame. Since strong relative outflow is never seen in this storm, the gust front speed is apparently about the same as the storm speed. Speed convergence of the airflow is evident in the area of the frontal discontinuity. The updrafts and high equivalent potential temperature values measured along and ahead of the gust front indicate warm, moist, low-level air is riding up over the gust front. The position of the large positive values of radial velocity in Fig. 3 suggests that the strongest inflow is actually above the gust front. Some mixing of the inflow air, which has a higher dew point temperature, with the outflow air as well as local acceleration of the low-level air is seen between 1405 and 1406 along the aircraft track near the precipitation area and below the main inflow. The inflow cloud structures (tail cloud and wall cloud) lie along and behind the gust front with cloud base at a height of about 0.7 km above the aircraft level.

Goff's model of the leading edge of a well-developed gust front with the airflow relative to the gust front is shown in Fig. 5. Although the gust front in this study is not as intense as some of those which Goff studied, a comparison can be made. The assumed position of the aircraft within the plane of the figure is shown for the period 1405–1410. Notice the implied downward mixing and high turbulence for the portion of the track between 1405 and 1406. This is evident from Fig. 4 as mentioned earlier and was probably enhanced in this case by the aircraft's nearness to the main precipitation area.

Mixing of rain-moistened outflow air with the inflow air at the upper boundary of the gust frontal surface appears to contribute to the production of the wall cloud in this storm. The *main* inflow through the tail cloud would consist of the low-level warm, moist environmental air which had ascended over the outflow boundary, however. The cool outflow air pushing under the inflow air may have contributed to the eventual weakening of the thunderstorm.

3. Conclusions

The low-level airflow and thermodynamic features of an intense hailstorm have been investigated with radar and research aircraft. The general low-level airflow at the base of the hailstorm has been determined, including the identification of a well-defined outflow air boundary. The inflow air is found to exist near and above the outflow air. The visually observed cloud features associated with the main updraft (the tail and wall clouds) have been found to occur just behind and above the outflow air boundary in this case. These results are in general agreement with the low-level structure as described for the storm scale by Browning and Foote (1975), and in the gust front scale by Goff (1976). It is comforting to confirm previous findings using a synthesis of two data systems that sense on markedly

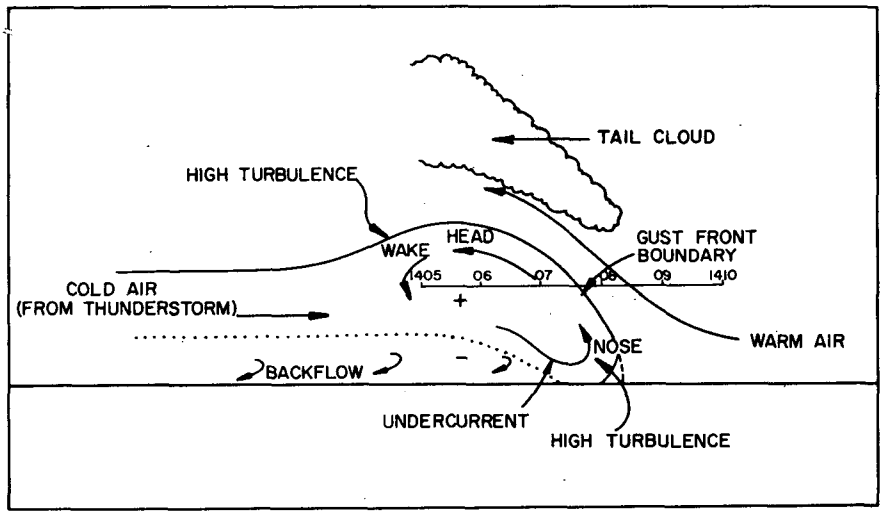

FIG. 5. The gust front model of Goff (1976). Winds are relative to the gust front motion. The aircraft track for 1405–1410 is shown as it would exist in the plane of the figure.

different ranges of meteorological scales. Furthermore, the addition of visible low-level features should aid in storm spotter warning procedures.

Acknowledgments. A large part of the data, including all of the radar data, were supplied by the National Severe Storms Laboratory. The National Center for Atmospheric Research funded by the National Science Foundation supplied the research aircraft and the processed aircraft data. This research was done as part of a graduate study program at the University of Oklahoma and was supported by the Atmospheric Research Section, National Science Foundation Grant ATM74-0340ba02, and by NOAA Grant 04-5-022-3.

REFERENCES

Brandes, E. A., 1977: Flow in severe thunderstorms observed by dual-Doppler radar. *Mon. Wea. Rev.*, **105**, 113–120.

Browning, K. A., and G. B. Foote, 1976: Airflow and hail growth in supercell storms and some implications for hail suppression. *Quart. J. Roy. Meteor. Soc.*, **102**, 499–533.

Fujita, T. T., 1957: A detailed analysis of the Fargo tornadoes of June 20, 1957. University of Chicago, Severe Local Storms Project Tech. Rep. No. 5, 29 pp.

Goff, R. C., 1976: Vertical structure of thunderstorm outflows. *Mon. Wea. Rev.*, **104**, 1429–1440.

Heymsfield, G. M., 1978: A dual-Doppler investigation of some kinematic and dynamic aspects of the Harrah tornadic storm. *Mon. Wea. Rev.*, **106** (in press).

Ray, P. S., 1976: Vorticity and divergence fields within tornadic storms from dual-Doppler observations. *J. Appl. Meteor.*, **15**, 879–890.